

Transport of clay particles and radioelements in a salinity gradient: experiments and simulations

M.-H. Fauré ^{a,*}, M. Sardin ^b, P. Vitorge ^a

^a *Section de GéoChimie, CEA, BP 6, F-92265 Fontenay-aux-Roses, France*

^b *Laboratoire des Sciences du Génie Chimique, CNRS-ENSIC, BP 451, F-54001 Nancy, France*

Received 17 December 1993; accepted 15 December 1994 after revision

Abstract

The problem of the transport of radioelements sorbed on colloids often occurs when assessing the safety of radioactive waste disposal. A methodology for studying the influence of particles on the transport of solute is proposed. A salinity gradient of NaCl is flowed through a chromatographic column filled with a mixture of sand and bentonite clay (5% by weight). As long as the NaCl concentration stays above a threshold value equal to 0.16 *M*, no particle migration out of the column is detected. A dramatic variation of the hydrodynamic properties of the column occurs just before the output of the clay particles: preferential pathways and dead water volumes are formed. The clay migration is first detected when NaCl concentration is < 0.16 *M*, and it is then controlled by varying NaCl concentration. For a given length and composition of the porous medium, the amount of clay that migrates depends only on the NaCl concentration of the feed solution. An empirical function is proposed to account for this. This function is included in a transport model to account for kinetic mass transfer between immobile and mobile water zones, and adsorption of trace solute such as cesium. The adsorption is assumed to be governed by cation exchange with sodium. This built model is in good agreement with the experimental results.

1. Introduction

The transport of radioelements in groundwaters is governed by water flow and by physicochemical interactions that determine the partition of radionuclides between the mobile phase and the stationary phase usually consisting of immobile water and reactive solid surfaces. The solubility of the radionuclides and their adsorption on the surface of

* Corresponding author.

porous media are usually involved in the mechanisms proposed to explain their retardation with respect to water motion. The reactive surface of a quartz porous medium is essentially due to the presence of fine minerals such as oxides or clays. The size of these fine particles is on the micrometric or submicrometric scale and they can be assimilated as colloids. The stability of these particles inside porous media (quartz, feldspar, calcite) is dependent on the water composition and in particular on its major cations. A change in salinity can drastically change the stability properties of the particles and induces a dispersion of these particles, so-called peptisation in soil science. These dispersed particles can plug porous media, they can also migrate and so, accelerate the transport of radionuclides in water (Buddemeier and Hunt, 1988).

Many studies have been devoted to this problem particularly in the field of petroleum and chemical engineering. Khilar and Fogler (1987) have presented an excellent review of the phenomena encountered when a salinity gradient occurs in low-permeability media.

The aim of this paper is to show that it is possible to monitor the transport of clay particles by flowing a salinity gradient of sodium chloride through a sand bed, and to quantitatively model the breakthrough curves of particles and associated radionuclides.

In this work, we first look for the parameters controlling particle release. After a study of the hydrodynamic characteristics, we develop a model to predict the clay particle migration in a salinity gradient. In the last part, we compare an experiment and its simulation of a cesium injection in a salinity gradient leading to the particle washout. Other examples and more details have been presented elsewhere (Fauré, 1994).

2. Experimental and methods

2.1. Experimental set-up

The experimental set-up (Fig. 1) is a liquid chromatographic system. Two pumps, fed by water or sodium chloride solution, and a gradient programmer allow us to decrease the NaCl concentration of the feed solution linearly with time. The solution of

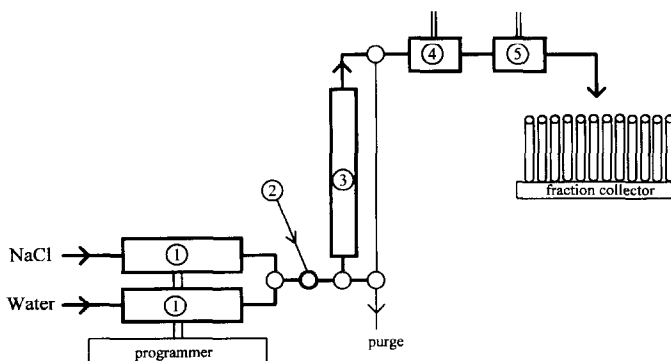


Fig. 1. Experimental set-up for the chromatographic technique (1 = pumps; 2 = injection loop; 3 = column; 4 = conductimeter cell; 5 = UV detector cell).

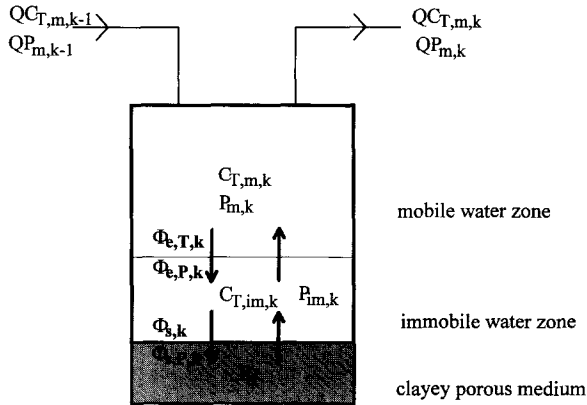


Fig. 2. Mixing-cell to model the transport with preferential pathways and dead volumes.

radioelement is injected with a 0.5-mL injection loop. A 16-mm-diameter column is filled with a mixture of dry sand and bentonite clay (5% by weight). The porous volume is 3 mL. The sand is 99% SiO₂ (Fauré, 1994); the clay is Foca 3[®], a montmorillonite type (Fauré, 1994); and cation exchange capacity (CEC), measured by injecting a ²²Na solution, is 71 meq/100 g (Fauré, 1994). At the outlet of the column, the NaCl concentration is controlled by conductivity. A UV (280 nm) cell measures the concentration of particles in the effluent. Samples are collected, and filtered (0.22 μm). The ¹³⁷Cs concentration in solution and fixed on the particles is deduced from γ-counting. The column is first purged of air with CO₂, and then saturated with an upward flow of sodium chloride 0.5 M at pH = 6.5. The flow rate is constant (1 cm³ min⁻¹).

2.2. Hydrodynamic measurement

The hydrodynamic properties of the column are measured initially and after every salinity change with tracer tests. The tracer test consists in injecting 0.5 mL of a 0.2 M NaCl solution on a column fed with a 0.5 M NaCl solution. The variations in conductivity are measured at the outlet of the column. The residence time distribution (RTD) so obtained (see Fig. 4) is corrected for input signal and dead volume due to the set-up (~ 0.6 mL). It is modelled by the classical model of mixing cells in series with exchange where the porous medium of the column, of porous volume V_p, is represented by J identical mixing cells in series (Villiermaux, 1981, 1982). Each cell (Fig. 2) contains the same fraction of water and solid phase. The water phase is divided into two zones where the composition is uniform: the mobile water zone of volume θ_mV_p/J, and the immobile water zone of volume θ_{im}V_p/J. The immobile water zone is in contact with the solid phase. The transport of a tracer for water is governed by its partition between the two water zones. The mass transfer between these two zones is assumed to be kinetically limited. Thus, the mass-balance equations for this tracer are:

(1) in mobile water,

$$QC_{m,k-1} = QC_{m,k} + \theta \frac{V_p}{J} \frac{dC_{m,k}}{dt} + \Phi_{e,k} \tag{1}$$

(2) in immobile water zone,

$$\theta_{\text{im}} \frac{V_p}{J} \frac{dC_{\text{im},k}}{dt} = \Phi_{e,k} \quad (2)$$

$C_{m,k}$ and $C_{\text{im},k}$ are the solute concentrations in the mobile and immobile water zone, respectively. As a first approximation, the flux, $\Phi_{e,k}$, is assumed to be controlled by a linear first-order kinetic law:

$$\Phi_{e,k} = \frac{\theta_{\text{im}} V_p}{J} \frac{C_{m,k} - C_{\text{im},k}}{t_M} \quad (3)$$

where t_M is the characteristic mass transfer time. In absence of convective flow in the immobile water zone, $\Phi_{e,k}$ is essentially due to a diffusion process (external and internal diffusion) and can be approximated by a formula given by Sardin et al. (1991). In the presence of convection, the mass transfer can be characterized by a recycling flow rate, q . A simple identification between the mass-balance equations leads to:

$$t_M = \frac{\theta_{\text{im}} V_p}{Jq} \quad (4)$$

The discrimination between these two approaches can be made by performing experiments at different flow rates. If t_M is constant whatever the flow rate value, the internal diffusion is predominant. In other cases, the mass transfer limitation can be due to different mechanisms: external diffusion, recycling flow, etc.

2.3. Salinity gradient experiment

The column is fed with a solution of sodium chloride whose concentration is decreased linearly ($dC/dV = cte$) from C_i to C_f within a volume, V_g , of solution. Then, the feed concentration is kept constant at C_f . The particle concentration is measured at the outlet of the column (Fig. 3). First, the column is fed with a NaCl solution whose concentration is C_i . Then, the NaCl concentration of the feed solution is decreased. During this decrease, the particles begin to leave the column. The particle concentration in the effluent increases as long as the NaCl concentration of the feed solution decreases. When the NaCl concentration is kept constant at C_f , the particle concentration decreases and vanishes. This typical experiment is reproducible from one column to another. It allows us to study the phenomenon of clay particle washout from porous media in a salinity gradient. Using this typical experiment, we find the parameters controlling the particle output in a salinity gradient in our experimental conditions.

3. Results and interpretation

3.1. Evolution of the hydrodynamics of the column

The particle movement in the column suggests that there are modifications to the flow properties. Accordingly, the hydrodynamic parameters of the porous medium have

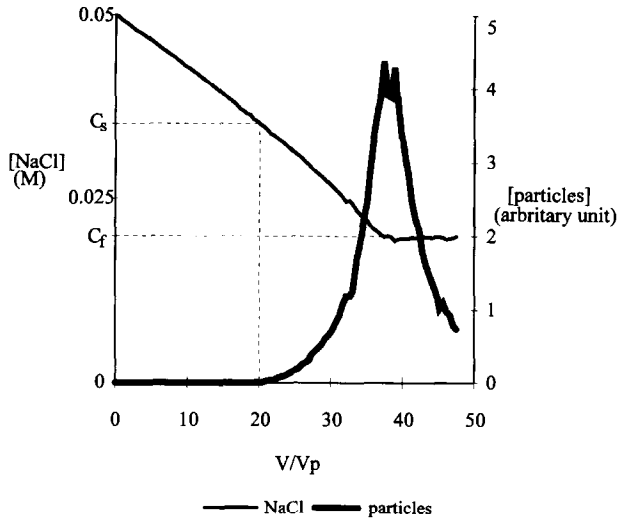


Fig. 3. Typical experiment: NaCl concentration of the feeding concentration decreases and particles go out of the column. NaCl and output of particles are shown here.

been measured after each salinity gradient experiment, independently of the particle output.

The column is first fed with a 0.5 M NaCl solution, then the concentration is instantaneously decreased down to C_g and it is kept constant during 10 mL, after it is increased up to 0.5 M. These experiments are repeated several times with injections for NaCl concentrations, C_g , of 0.2, 0.15, 0.1, 0.075 and 0.05 M. We check the evolution of the hydrodynamics of the porous medium, after each experiment, by means of the tracer test described in Section 2.2. The results are given in Fig. 4.

Initially, the breakthrough curve is symmetric: the water flow is almost a piston flow. As the NaCl concentration is decreased, the curve deforms from one experiment to the other. The maximum of the curve goes to smaller times and the weight of the tail increases. This indicates that preferential pathways and dead zones are created. The variations of the shape of the breakthrough curves start before the output of the clay particles.

According to the model, the NaCl decrease induces an increase of θ_{im} , the fraction of immobile water zone, and of t_M , the mass transfer time. We here measure the hydrodynamic parameters (J , θ_{im} , t_M) of the porous medium that has been fed with a NaCl solution of concentration, $C_g < 0.5$ M. But we do not know the J , θ_{im} , t_M variations as a function of NaCl concentration. This will be one of the major limitations of the prediction when modelling particle output.

3.2. Particle output

The particles begin to leave the column when the NaCl concentration of the feed solution becomes less than the threshold concentration, $C_s = 0.16$ M (Khilar and Fogler,

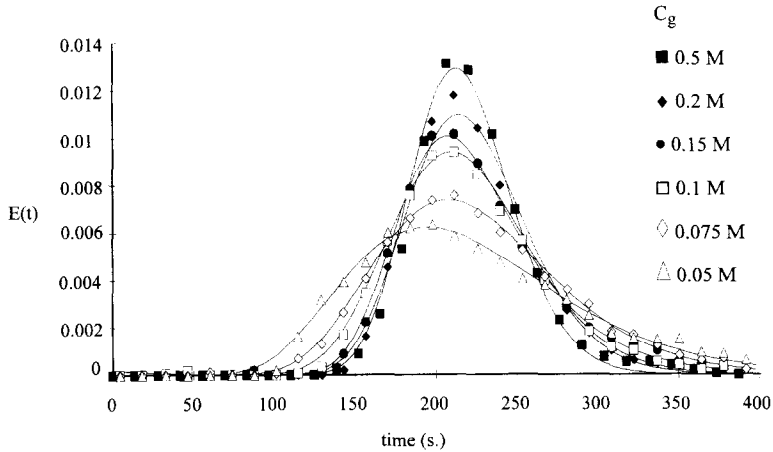


Fig. 4. Evolution of the hydrodynamic properties of the porous medium when $[\text{NaCl}]$ decreases. Numbers on the figure are C_g , the NaCl gap concentration (see text). The full drawn curves are simulated.

1984; Fauré, 1994) (Fig. 3). The amount of particles having left the column is only dependent on the values of the initial and final NaCl concentrations (C_i and C_f , respectively) of the feed solution. The particle concentration in the effluent depends on the volume, V_g , used to vary the NaCl concentration. It decreases while the volume, V_g , increases. To determine the limits of our measurements, some experiments have been made by varying other parameters (Fauré, 1994). The amount of particles that leave the column is dependent on the length of the porous medium and on the percentage of clay in the porous medium. On a column fed with NaHCO_3 and Na_2CO_3 solutions (pH = 8 and 10.8, respectively), the particle behaviour is the same but the NaCl threshold concentration is slightly different.

These observations show that all the particles do not move at the same NaCl concentration. When repeating a typical experiment, with the same initial and final NaCl concentration, no particle leaves the column: no more clay is available for the migration in this range of NaCl concentration. Experiments with a range of NaCl concentrations between 0.5 and 0.015 M show that the total amount of particles leaving the column is a function of NaCl concentration (Fig. 5). In this range, we find two domains where particles are able to leave the column. The first domain is from 0.16 to 0.05 M, and the second from 0.035 to 0.019 M. We then introduce the notion of particles available for migration, P_d , as a function of the NaCl concentration. $P_d(C_i) - P_d(C_f)$ is the amount of particles available for migration out of a new column when the NaCl concentration of the feed solution decreases from C_i to C_f . In order to model the particle output we will use this empirical function (Fig. 5).

4. Modelling the transport of particles and solutes in a salinity gradient

The previous experimental results show two points: (1) the amount of particles available, $P_d([\text{NaCl}])$, is a function of sodium chloride concentration; and (2) there are

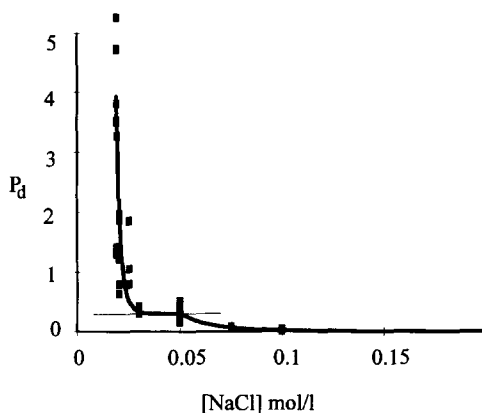


Fig. 5. Amount of particles available to migrate as a function of NaCl concentration: experimental point and empirical function $P_d([NaCl])$.

$[NaCl] > 0.16 M$	$P_d = 0$
$0.16 M \geq [NaCl] \geq 0.05 M$	$P_d = X_1(\exp([NaCl]^n) - \exp(0.16^n))$
$0.05 M \geq [NaCl] \geq 0.035 M$	$P_d = X_1(\exp(0.05^n) - \exp(0.16^n))$
$0.035 M \geq [NaCl] \geq 0.019 M$	$P_d = X_2[\exp([NaCl]^n) - \exp(0.035^n)] + P_d(0.05)$
$0.019 M \geq [NaCl]$	$P_d = X_2(\exp(0.019^n) - \exp(0.035^n)) + P_d(0.05)$
$n = -0.6, X_1 = 75,500$ and $X_2 = 7,970$	

some interactions between the particles and the porous medium. Among these interactions, we already know the kinetic limitation of particle transfer out of the immobile water zone. The contribution of the other interactions, such as filtration by the porous medium, should be included in the P_d function. A phenomenological model of transport must include these features. The assumptions of the model are as follows:

(1) The water phase is divided into two zones: a mobile water zone where particles migrate at the water flow velocity and an immobile water zone where the particles coming from the solid surface are available for mass transfer between the mobile and immobile water zones.

(2) The mass transfer between the two zones is assumed to be limited by a first-order law. The characteristic mass transfer time is t_{M_s} .

(3) The amount of particles available from the porous medium is only a function of sodium chloride concentration, $P_d([NaCl])$.

(4) The transport in the mobile zone is convective–dispersive and can be modeled by a series of mixing cells (Fig. 2).

The particle mass balance in the mobile water zone, similar to that of the solute, is:

$$QP_{m,k-1} = QP_{m,k} + \frac{\theta_m V_p}{J} \frac{dP_{m,k}}{dt} + \Phi_{e,P,k} \quad (5)$$

But in immobile water zone, we add the particle source term:

$$\frac{\theta_{im} V_p}{J} \frac{dP_{im,k}}{dt} - \Phi_{s,P,k} = \Phi_{e,P,k} = \frac{\theta_{im} V_p}{J} \frac{P_{m,k} - P_{im,k}}{t_{M_p}} \quad (6)$$

$\Phi_{s,P,k}$ is the source term of particles from the porous medium to the immobile water zone. It is calculated from the $P_d([\text{NaCl}])$ function:

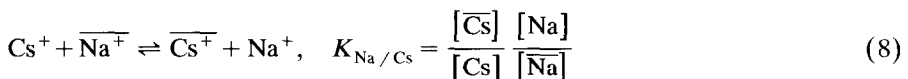
$$\Phi_{s,P,k} = \frac{M}{J} \frac{dP_d}{dt} = \frac{M}{J} P'_d \frac{d[\text{NaCl}]}{dt} \quad (7)$$

where P'_d is the derivative of $P_d([\text{NaCl}])$ with respect to $[\text{NaCl}]$. The value of $\Phi_{s,P,k}$ is, thus, directly a function of the time derivative of $[\text{NaCl}]$. Cl^- is considered as a tracer for water, Na^+ is the major cation in solution so $[\text{NaCl}] \approx [\text{Cl}^-]$ and, $d[\text{NaCl}]/dt$ is a solution of the two mass equations (1) and (2) for the tracer (see Section 2.2). These two mass-balance equations, Eqs. 5 and 6, of particles introduce a characteristic mass transfer time for particles, t_{M_p} .

The validity of this model has been tested on a set of experiments of clay destabilisation where the only cation is Na^+ . For each destabilisation experiment, the porous volume, V_p , the number of cells, J , the fraction of immobile water zone, θ_{im} , and t_M are initially measured by the tracer test. These values are used in the simulations. The transfer times, t_M and t_{M_p} , are dependent on the hydrodynamic characteristics of the porous medium. For each domain of destabilisation, t_{M_p} is fitted on the results of one typical experimental. This shows that for a given range of salinity gradient the values of t_M and t_{M_p} are relatively constant (Table 1). An example of simulation of particle motion is given in Fig. 6 together with experimental results. The prediction is very good confirming the phenomenological validity of the model.

4.1. Adsorption of solute

We here use cesium, examples with calcium and neptunium(V) are given elsewhere (Fauré, 1994). Cesium is assumed to be adsorbed on the porous medium through cation exchange with sodium:



$[\overline{\text{Cs}}]$ and $[\overline{\text{Na}}]$ are the concentration of cesium and sodium, respectively, on the surface of the porous medium in moles per kg of solid.

At trace level $[\text{Cs}] \ll [\text{Na}]$ and $[\overline{\text{Cs}}] \ll [\overline{\text{Na}}]$. Consequently, the electroneutrality

Table 1

Hydrodynamic parameters (J , θ_{im} , t_M , t_{M_p}) used to simulate output of particles in each NaCl concentration field of destabilisation

	Field 1 [NaCl] = 0.16–0.05 M	Field 2 [NaCl] = 0.035–0.019 M
J	51	15
θ_{im}	0.125	0.285
t_M	0.05 τ	0.09 τ
t_{M_p}	12 τ	20 τ

relationships in the phase is: $[Na] \approx [Cl]$ and $[\overline{Na}] \approx [CEC]$. Thus for a given $[Cl]$, the distribution coefficient of cesium is constant:

$$\frac{[\overline{Cs}]}{[Cs]} = K_{Na/Cs} \frac{[CEC]}{[Cl]} \tag{9}$$

(1) Without particle motion, in a porous medium, the cesium mass-balance equation in the mobile zone is obtained by substituting the tracer for Cs^+ in Eq. 1, but the equation in immobile water zone is:

$$\frac{d[Cs]_{im,k}}{dt} + \frac{M}{\theta_{im} V_p} \frac{d[\overline{Cs}]_{im,k}}{dt} = \frac{[Cs]_{m,k} - [Cs]_{im,k}}{t_M} \tag{10}$$

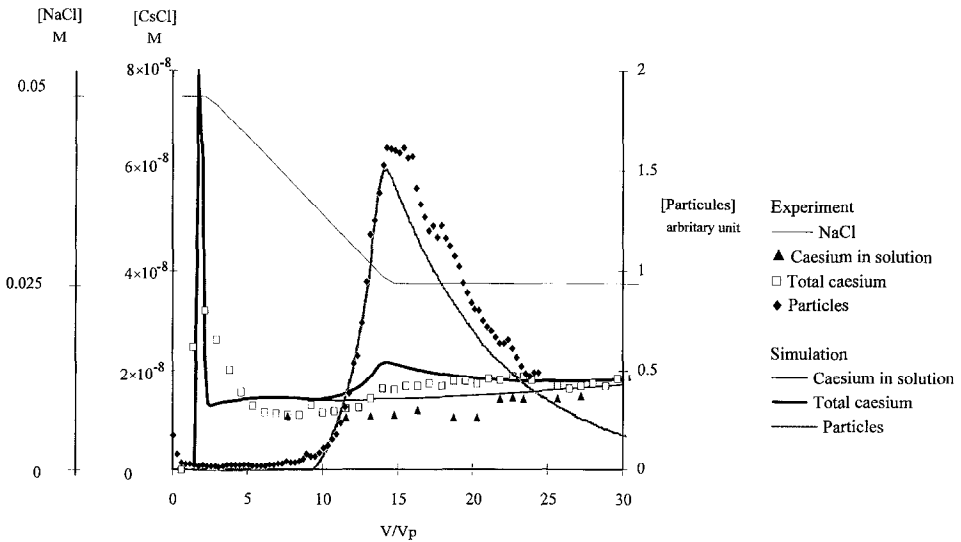


Fig. 6. Cesium and particle migration. Experiment and simulation of a 0.5-mL injection of a $5 \cdot 10^{-5}$ M CsCl–0.05 M NaCl solution with decrease of the feeding solution from 0.05 to 0.02 M and output of particles. The plots are experimental data and the full drawn curves are simulated. The preferential pathways and ionic exchange process explain the initial Cs peak. Whereas the second increase of Cs concentration is due to Cs transport on the clay particles (see text).

If we assume state of equilibrium between the Cs^+ in the immobile water zone and the adsorbed cesium:

$$[\overline{\text{Cs}}]_{\text{im},k} = K_{\text{Na/Cs}} \frac{[\text{CEC}]}{[\text{Cl}]} [\text{Cs}]_{\text{im},k} \quad (11)$$

In absence of a salinity gradient $[\text{Cl}]$ is constant, thus substituting $[\overline{\text{Cs}}]_{\text{im},k}$ for Eq. 11 into Eq. 10 one obtains:

$$\frac{d[\text{Cs}]_{\text{im},k}}{dt} = \frac{[\text{Cs}]_{\text{m},k} - [\text{Cs}]_{\text{im},k}}{t_M} \left/ \left(1 + \frac{M}{\theta_{\text{im}} V_p} \frac{[\text{CEC}]}{[\text{Cl}]} K_{\text{Na/Cs}} \right) \right. \quad (12)$$

If $[\text{Cl}]$ varies:

$$\begin{aligned} \frac{d[\text{Cs}]_{\text{im},k}}{dt} & \left(1 + \frac{M}{\theta_{\text{im}} V_p} K_{\text{Na/Cs}} \frac{[\text{CEC}]}{[\text{Cl}]_{\text{im},k}} \right) \\ & = \frac{[\text{Cs}]_{\text{m},k} - [\text{Cs}]_{\text{im},k}}{t_M} + \frac{M}{\theta_{\text{im}} V_p} K_{\text{Na/Cs}} \frac{[\text{CEC}]}{[\text{Cl}]_{\text{im},k}^2} [\text{Cs}]_{\text{im},k} \frac{d[\text{Cl}]_{\text{im},k}}{dt} \end{aligned} \quad (13)$$

Eq. 13 shows that the accumulation of Cs^+ in the immobile zone ($d[\text{Cs}]_{\text{im},k}/dt$) is dependent on $[\text{Cl}^-]$ (ionic exchange process with Na^+) and on its derivative (gradient).

The salinity gradient being not too steep, the integration of the set of four ordinary differential equations is easily resolved numerically.

(2) *The presence of mobile particles* adds supplementary terms. In the mobile water zone, the mass balance for Cs^+ becomes:

$$Q[\text{Cs}]_{\text{T,m},k-1} = Q[\text{Cs}]_{\text{T,m},k} + \frac{\theta_{\text{m}} V_p}{J} \frac{d[\text{Cs}]_{\text{T,m},k}}{dt} + \Phi_{\text{e,CsT},k} \quad (14)$$

$\Phi_{\text{e,CsT},k}$ is the mass flux of total cesium between the mobile and immobile water zone. Its expression takes into account the different characteristic times, t_M and t_{M_p} (see Eq. 18):

$$[\text{Cs}]_{\text{T,m},k} = [\text{Cs}]_{\text{m},k} + [\text{Cs}]_{\text{p,m},k} \quad (15)$$

$[\text{Cs}]_{\text{p,m},k}$ is the concentration of Cs^+ on particles in the mobile water zone:

$$[\text{Cs}]_{\text{p,m},k} = K_{\text{Na/Cs}} \frac{[\text{CEC}]_p}{[\text{Cl}]} [\text{Cs}]_{\text{m},k} P_{\text{m},k} \quad (16)$$

Eqs. 15 and 16 give:

$$[\text{Cs}]_{\text{T,m},k} = [\text{Cs}]_{\text{m},k} \left[1 + K_{\text{Na/Cs}} \frac{[\text{CEC}]_p}{[\text{Cl}]} P_{\text{m},k} \right] \quad (17)$$

Note that Eq. 17 is also valid in the immobile water zone (equilibrium assumption in each zone). Consequently, we can use the total concentration of Cs^+ in immobile water zone:

$$\begin{aligned} & \frac{\theta_{\text{im}} V_p}{J} \frac{d[\text{Cs}]_{\text{T,im},k}}{dt} + \Phi_{\text{s,CsT},k} \\ & = \frac{\theta_{\text{im}} V_p}{J} \left[\frac{[\text{Cs}]_{\text{m},k} - [\text{Cs}]_{\text{im},k}}{t_M} + \frac{[\text{Cs}]_{\text{p,m},k} - [\text{Cs}]_{\text{p,im},k}}{t_{M_p}} \right] \end{aligned} \quad (18)$$

$\Phi_{s,Cs_T,k}$ is the flux of free cesium from the porous medium (Eq. 9 or its derivative depending on the case). The use of Eq. 16 applied to the immobile zone and Eq. 18 allows us to eliminate $[Cs]_p$.

The set of differential equations are solved numerically. The Fig. 6 illustrates the ability of the model to describe the behaviour of a complex system where particles and solutes are mobile in a salinity gradient. The parameters used in the model are not fitted, they are determined from independent experiments.

4.2. Experiment

The column is saturated with a 0.05 M NaCl solution. A 0.5 mL $5 \cdot 10^{-5}$ M CsCl–0.05 M NaCl solution is injected. The NaCl concentration of the feed solution decreases from 0.05 to 0.025 M during $10.9V_p$. These conditions are chosen to induce Cs^+ transport on clay particles and to couple it with Na^+/Cs^+ exchange process. Concentrations of particles, and cesium in solution and fixed on particles are measured at the outlet of the column (Fig. 6). This experiment is simulated with the hydrodynamic parameters $J = 15$, $\theta_{im} = 0.285$, $t_M = 0.09\tau$ and $t_{M_p} = 20\tau$ (τ is the mean residence time of the tracer for water; $\tau = V_p/Q$).

Cesium concentration starts to increase immediately at the first V_p after the injection because of the presence of preferential pathways in the porous medium. While the Na^+ concentration is maintained constant at 0.05 M, the Cs^+ concentration increases. When the NaCl concentration of the feed solution begins to decrease, we see that the CsCl concentration in the effluent also decreases. Then it increases again when particles begin to leave the column. This first cesium peak is due to preferential pathways and competition between sodium/cesium for sorption. When the NaCl concentration decreases, the cesium concentration in the effluent decreases because it is more retained on the porous medium. The second increase of cesium concentration is due to the migration of clay particles on which cesium is fixed. The simulation of the beginning of the breakthrough cesium curve is not very good because it is difficult to estimate the hydrodynamic parameter and we do not consider an internal mass transfer time. The simulation also shows an increase of cesium concentration due to particles in good agreement with the experiment.

5. Conclusions

Our methodology uses reproducible experiments, simulations and experimental verification. It could be used for other kinds of colloids and different porous media. The particles indeed influence the solute breakthrough curves because cations can be transported by particles. Still the particle migration occurs only in special physico-chemical conditions. The movement of particles induces dramatic changes in the hydrodynamic properties of the porous medium such as preferential pathways and dead volumes. To model the transient transport of particles and solute in a gradient salinity, we couple steady flow, ionic exchange process and we use the P_d function of particles available for migration as a function of NaCl concentration. This empirical function P_d

depends on the porous medium (length, proportion of clay, pH, etc.), and points out which of its specific properties should be characterized and could be better understood as a result of further theoretical and experimental studies.

6. Notation

$\overline{[X]}$	concentration of solute sorbed (mol/kg of porous medium)
$[X]$	concentration of free ion X^{z-} in solution (mol L ⁻¹)
$[X]_T$	total concentration of ion X^{z-} in solution: sum of free ions and of ions sorbed on particles (Eq. 15) (mol L ⁻¹)
$C(t)$	concentration of solute (M)
C_i, C_f	initial and final NaCl concentrations, respectively, of the decrease of salinity (M)
C_g	NaCl concentration of a gap injection (M)
$C_{m,k}, C_{im,k}$	concentration of solute in the mobile and “immobile” water phase, respectively, in the k th cell (M)
$C_{P,m,k}, C_{P,im,k}$	concentration of solute fixed on the particles in the mobile and immobile water zones, respectively (M)
$[CEC]$	cation exchange capacity of the porous medium (mol kg ⁻¹)
$[CEC]_p$	CEC of the clay particle; $[CEC]_p = [CEC]/(\%$ of the weight clay in porous medium) (M)
$E(t_s)$	residence time distribution
J	number of mixing cells
$K_{Na/Cs}$	equilibrium constant of the reaction of Na/Cs ion exchange
M	porous medium weight in the column (kg)
P_d	kg of particles available to migrate as a function of NaCl concentration per kg of porous medium
P'_d	derivative of P_d with respect to $[NaCl]$

Q	flow rate of the column feed solution ($L s^{-1}$)
q, q_p	solute and particle flow rate, respectively, between the mobile and immobile water zones ($L s^{-1}$)
t_M	characteristic solute mass transfer time (s)
t_{M_p}	characteristic particles mass transfer time (s)
V_p	volume accessible to the fluid: porous volume (L)
V_g	volume of feed solution used to decrease the NaCl concentration from C_i to C_f (L)
Φ_e	flux between mobile and immobile water zones ($mol s^{-1}$)
Φ_s	flux between immobile water zone and porous medium ($mol s^{-1}$)
θ_m, θ_{im}	fraction of mobile and immobile water, respectively ($\theta_m + \theta_{im} = 1$)
τ	mean residence time of a tracer for water $\tau = V_p/Q$ (s)

References

- Buddemeier, R.W. and Hunt, J.R., 1988. Transport of colloidal contaminants in groundwater: radionuclide migration at the Nevada Test Site. *Appl. Geochem.*, 3: 535–548.
- Fauré, M.-H., 1994. Migration de particules et de solutés en milieu poreux — Modélisation du transport simultané de particules argileuses et de radionucléides sous l'effet d'un gradient de salinité. Thèse, Institut National Polytechnique de Lorraine, Nancy.
- Khilar, K.C. and Fogler, H.S., 1984. The existence of a critical salt concentration for particle release. *J. Colloid Interface Sci.*, 101(1): 214–224.
- Khilar, K.C. and Fogler, H.S., 1987. Colloidally induced fines migration in porous media. *Rev. Chem. Eng.*, 4(1/2): 41–109.
- Sardin, M., Schweich, D., Leij, F.J. and van Genuchten M.Th., 1991. Modeling non-equilibrium transport of linearly interacting solutes in porous media: a review. *Water Resour. Res.*, 27(9): 2287–2307.
- Villiermaux, J., 1981. Theory of linear chromatography. In: A.E. Rodrigues and D. Tondeur (Editors), *Percolation Processes: Theory and Applications*. NATO (N. Atlantic Treaty Org.) ASI (Adv. Stud. Inst.) Ser. E, Vol. 33. Sijthoff and Noordhoff, Rockville, MA.
- Villiermaux, J., 1982. Génie de la réaction chimique: Conception et fonctionnement des réacteurs. Lavoisier Tech-doc, Paris, 401 pp.